

# Compact and Planar WCDMA/WLAN/UWB Antenna with Shorted Loop and Monopole Elements

**Bahadır S. Yıldırım<sup>1</sup>, Erkul Başaran<sup>2</sup>, and Bahattin Türetken<sup>3</sup>**

<sup>1</sup>Department of Electrical and Electronics Engineering  
Muğla Sıtkı Koçman University, Muğla, 48000, Turkey  
bahadır.yildirim@mu.edu.tr

<sup>2</sup>Department of Electrical and Electronics Engineering  
Piri Reis University, Tuzla, İstanbul, 34940, Turkey  
ebasaran@pirireis.edu.tr

<sup>3</sup>Department of Electrical Engineering  
University of Karabük, Karabük, Turkey  
bahattinturetken@karabuk.edu.tr

**Abstract** — A compact, planar, multiband antenna with loop and monopole elements suitable for wideband code division multiple access (WCDMA), wireless LAN (WLAN), and ultra wideband (UWB) wireless communications is presented in this paper. The antenna was built on FR4-type substrate and fed by a microstrip transmission line for easy integration with RF/microwave circuitry on the same circuit board. The physical low-band of the antenna includes 1.9–2.17-GHz WCDMA and 2.45-GHz WLAN bands, whereas the high-band spans from about 3.3 to about 11-GHz including 5-GHz WLAN, 3.1–10.6-GHz UWB, and 4–8-GHz C bands. Antenna  $S_{11}$  and radiation pattern measurements are presented. It's shown that measurements and simulations are in good agreement.

**Index Terms** — Antenna measurements, electromagnetic analysis, mobile antennas, wideband antennas.

## I. INTRODUCTION

A compact and multiband antenna with planar loop and monopole elements printed on FR4-type substrate has been presented in this paper for wideband code division multiple access (WCDMA), wireless LAN (WLAN), and ultra wideband (UWB) wireless communications. Various loop-type antennas have been reported in the literature. These include a loop-type antenna with an L-shaped section operating for the 3–5.1-GHz section of the UWB spectrum [1], a vertically mounted loop-type antenna on a mobile phone printed circuit board (PCB) for the 3–6-GHz band [2], a capacitively-loaded loop antenna for mobile handsets suitable for 900/1800/1900/2100 MHz mobile and 2.45/5-GHz WLAN bands [3], and a loop antenna for

2.45-GHz WLAN band [4]. Unlike the antennas described in [1–4], the presented antenna offers a significantly wider bandwidth spanning from 1.9 to 2.6-GHz and then from about 3.3 to 11-GHz. For applications requiring full UWB spectrum of the 3.1–10.6-GHz band, a loop antenna with a complex CPW/CPS type transition [5] has been reported. However, the presented antenna is multiband, provides a 2.1-GHz WCDMA band in addition to the UWB band, and does not require a complex CPW/CPS transition for feeding the antenna. A CPW-fed half loop-type antenna operating from about 3 to 20-GHz [6] has also been reported. The presented antenna offers multiband operation including 2.1-GHz WCDMA functionality, and the size of its footprint is less than half than that of the antenna described in [6]. All these antennas [1–6] have a single loop element to generate the desired band whereas the presented antenna is a multi-element antenna. Multi-element antennas including loop and monopole elements have also been reported for GSM850/900 and GSM1800/1900/UMTS functionality of laptops [7]. The presented antenna differs from [7] by its WCDMA and UWB functionality.

The motive behind the presented antenna is to achieve a compact WCDMA/UWB antenna which can be integrated with RF/microwave circuitry on the same board. The antenna employs microstrip technology and a shorted loop-type element with a tapered feed to generate the wideband response as opposed to tapered monopole structures which are commonly used as classical wideband radiators. In addition, 2.1-GHz WCDMA and 2.45-GHz WLAN functionalities have been included using an L-shaped monopole element. Basically, the antenna has two physical bands; the lower band spans from about 1.9 to 2.6-GHz, and the high

band spans from about 3.3 to 11-GHz. The low-band accommodates the 1.9–2.17-MHz WCDMA and the 2.45-GHz WLAN bands whereas the high band includes the 3.1–10.6-GHz UWB, 5-GHz WLAN, and 4–8-GHz C bands. The presented antenna has a footprint of 25×25-mm<sup>2</sup> and is compact enough to be integrated with RF circuitry on the same circuit board. Multiband UWB antennas with smaller footprints exist and one such example has been reported in [8] which uses a diamond-shaped monopole with notches. However, the design reported in [8] does not provide WCDMA functionality. Analysis of the presented antenna was carried out using extensive full-wave electromagnetic simulations with Ansoft HFSS [9] and CST Microwave Studio [10]. Antenna  $S_{11}$  and radiation pattern measurements are presented to validate the simulations.

**II. ANTENNA DESIGN**

**A.  $S_{11}$  measurements and simulations**

The antenna was built on 62×64×1 (mm<sup>3</sup>) FR4 substrate using microstrip technology. Antenna geometry and a photograph of the fabricated antenna are shown in Fig. 1 and Fig. 2, respectively. The substrate material FR4 whose relative dielectric constant and loss tangent are 4.4 and 0.02, respectively, has been preferred over other substrates because it is a low-cost and widely available material.

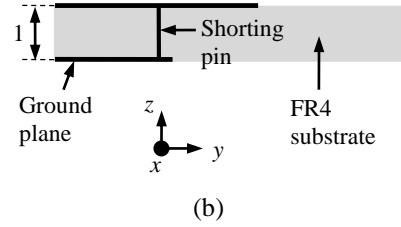


Fig. 1. Geometry of the antenna. All dimensions are in millimeters.

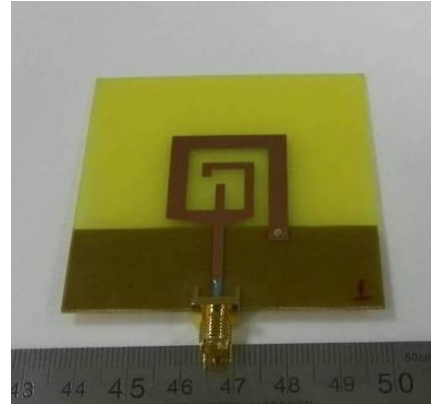
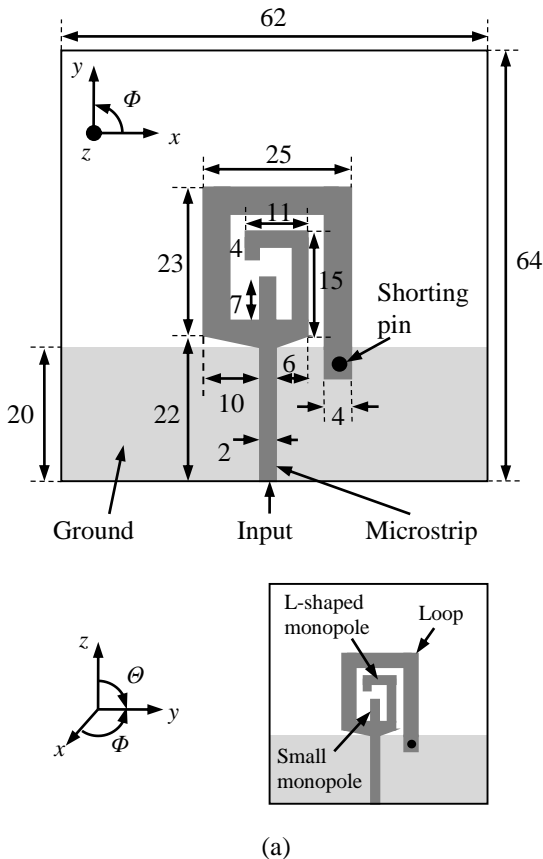


Fig. 2. Photograph of the fabricated antenna.



The antenna has three radiating elements as shown in Fig. 1 (a). Of these, the rectangular loop shaped element with tapered feed is shorted to the RF ground through a shorting pin. High-band response is primarily due to the shorted loop and the coupling between the shorted loop and monopoles. The low-band is generated primarily by the L-shaped monopole, and also due to the coupling between the L-shaped monopole and the loop. The L-shaped monopole resonates at about  $0.5\lambda$ , whereas the loop resonates at about  $1\lambda$ . First loop resonance is around 1.94-GHz. However, this resonance is weak in the sense that it does not produce a usable  $S_{11}$  bandwidth. The small monopole element improves matching from about 6 to 8-GHz. The width of the loop and monopole elements are 4-mm and 2-mm, respectively. These elements are fed by a 2-mm wide 50- $\Omega$  microstrip line. The transition from the feeding microstrip to the antenna has been tapered to improve the high-band matching. During the simulations, the shorting pin has been modeled as a 1.2-mm diameter copper tube, and top and bottom layer copper metallization has a thickness of 0.035-mm. For the fabricated antenna, a 1-mm diameter hole was drilled after the fabrication and filled with a conductive fluid which became solid after a while.

Antenna  $S_{11}$  measurements have been performed at TÜBİTAK (The Scientific and Technological Research Council of Turkey) BİLGEM (Center of Research for Advanced Technologies of Informatics and Security)

Antenna Test and Research Center using an Agilent E8362C 20-GHz PNA microwave network analyzer. Comparison of measured and simulated  $S_{11}$  responses of the antenna is shown in Fig. 3. Measurement and simulations agree well up to about 9.5-GHz. Above 9.5-GHz, measurement does not meet the industry standard -10 dB specification though it's still better than -6 dB up to 11-GHz. This problem may be due to the build quality of the SMA connector, fabrication process, substrate loss, and the shorting pin. Figure 4 shows the HFSS simulated effect of the SMA connector on the  $S_{11}$  response of the antenna from 7 to 11-GHz. It can be seen that there are slight variations in  $S_{11}$  response when the connector is present but no major variations exist. HFSS simulated effect of the short on the  $S_{11}$  response of the antenna has also been investigated by placing a 2.5-mm gap between the shorting pin and the loop to make the loop "open". Figure 5 shows that when the loop is open, the antenna does not have the low-band and the high-band starts from about 4.2-GHz.

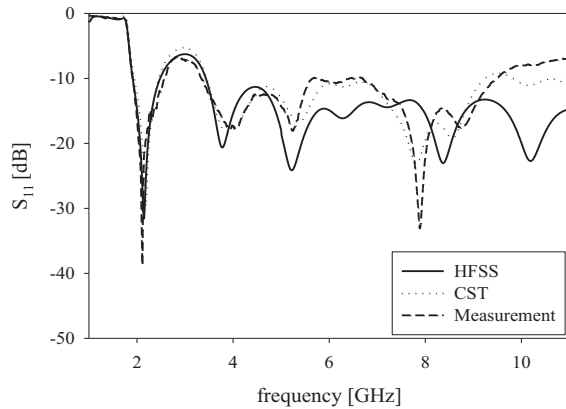


Fig. 3. Measured and simulated  $S_{11}$  response of the antenna.

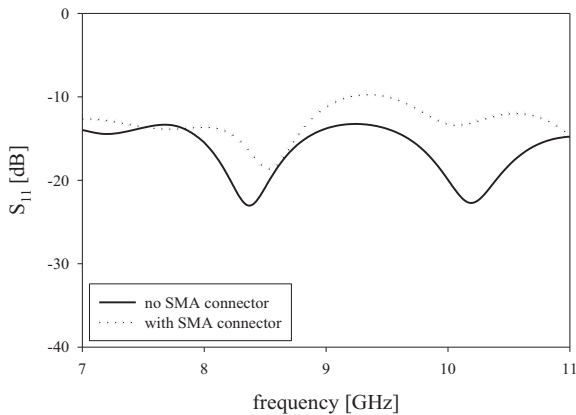


Fig. 4. Effect of the SMA connector on the  $S_{11}$  response of the antenna.

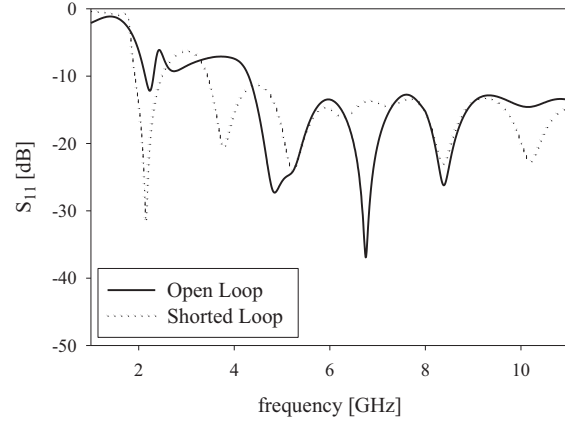


Fig. 5. Effect of the short on the  $S_{11}$  response of the antenna.

## B. Radiation pattern measurements and simulations

Antenna radiation pattern measurements were performed at TÜBİTAK BİLGEM Antenna Test and Research Center using a wideband double-ridged horn antenna as the probe antenna. The distance between probe and test antennas was about 2.6 meters. The antenna is placed on a positioner that turns only from  $0^\circ$  to  $\pm 160^\circ$ . For this reason, some measurement points were not available. Radiation patterns of the antenna at 2.1, 5.3, 8.1, and 10-GHz are shown in Figs. 6-9, respectively. The coordinate system for the indicated planes are shown in Fig. 1. For the  $xy$  plane radiation pattern, azimuth angle  $\phi$  varies, whereas the elevation angle  $\theta$  is set to  $90^\circ$ . For the  $xz$  plane radiation pattern,  $\theta$  varies and  $\phi=0^\circ$ .

The probe antenna was in vertical polarization. Vertically polarized patterns have been measured in  $xy$  and  $xz$  planes, according to the coordinate system shown in Fig. 1. The peak antenna gains at 2, 5.3, 8.1, and 10-GHz are 2, 4.4, 3.3, and 4-dBi, respectively. The pattern exhibits many lobes at higher frequencies due to complex current distribution on the radiating element. The radiation pattern measurements are in very good agreement with CST and HFSS simulations. Slight discrepancies can be due to RF currents that are re-radiated by the feeding coaxial cable of the antenna and issues related to antenna alignment and positioning.

Antenna realized gain simulations by HFSS and gain measurements are shown in Fig. 10 at 2.1, 5.3, 8.1, and 10-GHz. Realized gain is the power gain of the antenna including mismatch losses. Since the antenna is driven through a microstrip transmission line, effect of this line has also been included in the realized gain. It can be observed from Fig. 10 that measured gain is about 1.0-dB higher than the simulated gain. This difference may be due to calibration issues related to anechoic

antenna chamber. The antenna has a good gain characteristic across the desired frequency range.

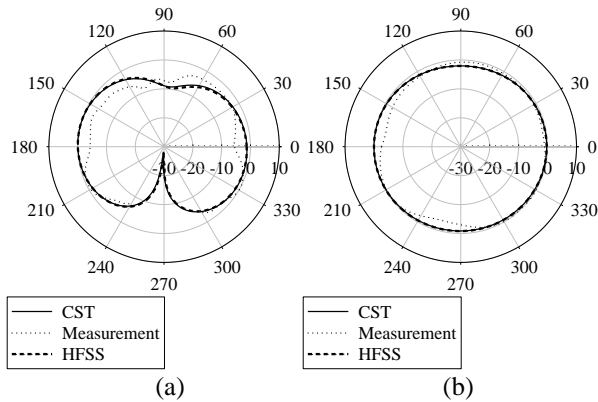


Fig. 6. Radiation pattern at 2.1-GHz in: (a)  $xy$  and (b)  $xz$  planes.

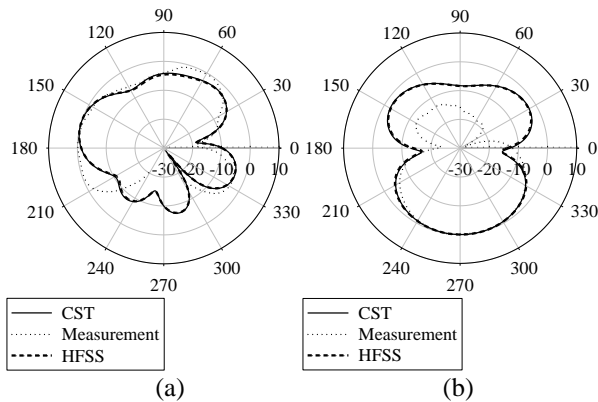


Fig. 7. Radiation pattern at 5.3-GHz in: (a)  $xy$  and (b)  $xz$  planes.

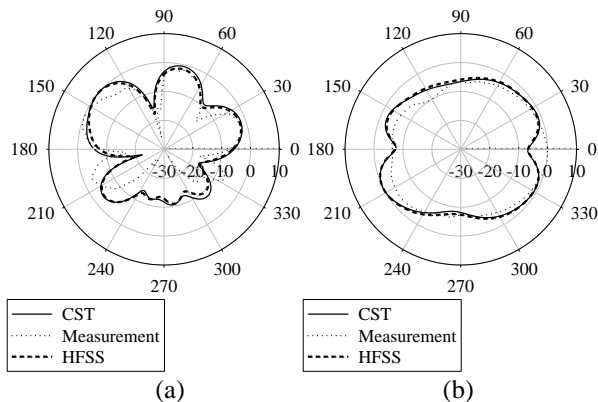


Fig. 8. Radiation pattern at 8.1-GHz in: (a)  $xy$  and (b)  $xz$  planes.

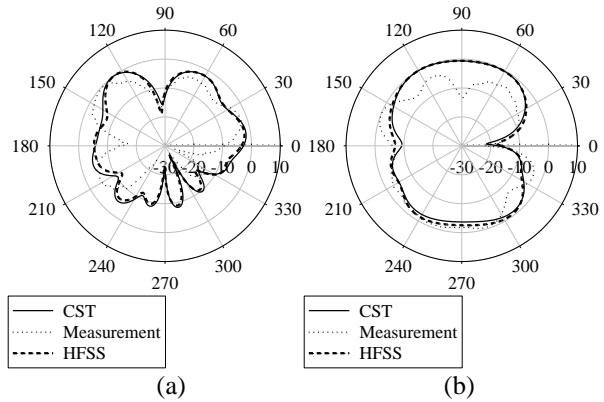


Fig. 9. Radiation pattern at 10-GHz in: (a)  $xy$  and (b)  $xz$  planes.

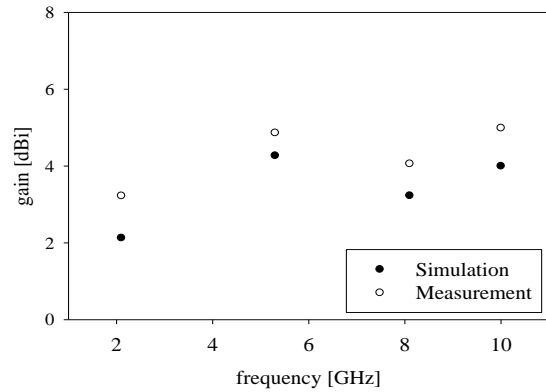
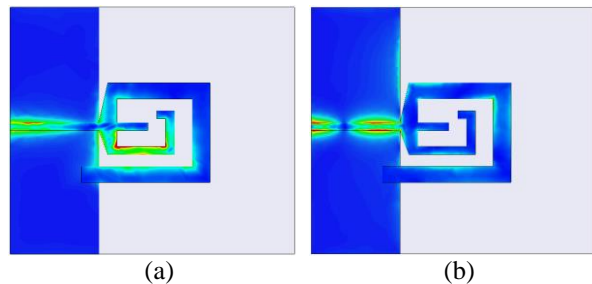


Fig. 10. Measured and simulated antenna gain.

Simulated surface current densities at 2.1, 5.3, 8.1, and 10-GHz are shown in Fig. 11. The maximum scale for each plot is the same. The L-shaped monopole has high current density and appears very active at 2.1-GHz as shown in Fig. 11 (a). At 5.3-GHz the loop is more active as shown in Fig. 11 (b). Figure 11 (c) shows that all elements are active at 8.1-GHz. Since there are three radiating elements, there is always some coupling among them, and the frequency response of the antenna is a result of these complex interactions.



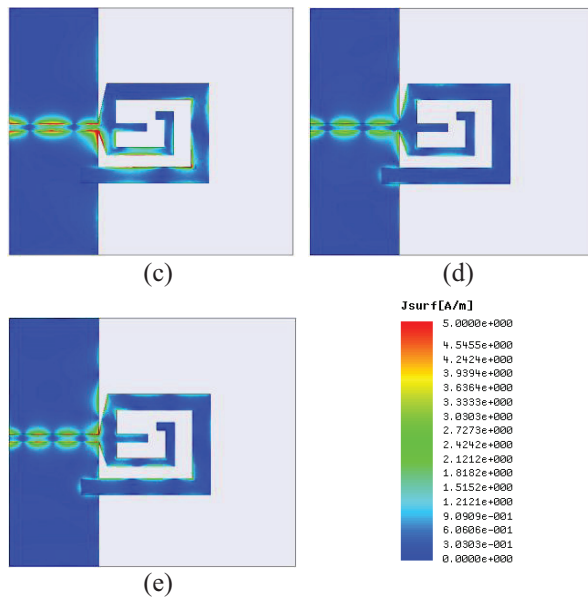


Fig. 11. Simulated surface current densities at: (a) 2.1-GHz, (b) 5.3-GHz, (c) 8.1-GHz, (d) 10-GHz, and (e) 12-GHz. Color scale is from 0 A/m to 5 A/m.

### III. CONCLUSION

The presented antenna is compact, wideband, planar, and multiband. The bandwidth spans from about 1.9 to 2.6-GHz, and then from about 3.3 to 11-GHz. Thus, it is suitable for WCDMA, WLAN, UWB, and C band applications. Primary difference between this design and the other UWB antennas is the use of a shorted loop element. UWB response is primarily due to the shorted loop and the coupling between the shorted loop and monopoles, whereas the other UWB antennas use tapered monopoles as their radiating element. The presented antenna exhibits good impedance and gain behavior. Because of its compact size and the microstrip technology, it can be integrated with RF/microwave circuitry on the same board easily.

### ACKNOWLEDGMENT

The authors thank to Eren Akkaya and Fatma Zengin at TÜBİTAK BİLGEM Antenna Test and Research Center for their help with radiation pattern and gain measurements.

### REFERENCES

- [1] K. Y. Yazdandost and R. Kohno, "Ultra wideband L-loop antenna," *IEEE International Conference on Ultra-Wideband*, pp. 201-205, 2005.
- [2] M. Kawakatsu and V. Dmitriev, "A compact and simple loop-type planar antenna for broadband applications," *IEEE MTT-S International Microwave and Optoelectronics Conference*, pp. 159-162, 2009.
- [3] Y. Shih, B. Wang, Y. Lu, J. Cheng, S. Chen, and P. Hsu, "Capacitively-loaded loop antenna for multi-

band mobile handsets," *Proceedings of Int. Workshop on Antenna Technology*, pp. 239-242, 2008.

- [4] A. Chen, C. Tang, and Z. Lu, "A loop antenna for WLAN application," *Proceedings of Asia Pacific Microwave Conference*, vol. 2, 2005.
- [5] S. Mao and S. Chen, "Frequency- and time-domain characterizations of ultrawideband tapered loop antennas," *IEEE Trans. Antennas and Propag.*, vol. 55, no. 12, pp. 3698-3701, December 2007.
- [6] Y. Lee, C. Wang, and J. Sun, "A new half-loop antenna for UWB spectrum," *Proceedings of Asia Pacific Microwave Conference*, pp. 1987-1989, 2006.
- [7] Y. Chi, T. Chiu, and F. Hsiao, "Printed penta-band laptop computer antenna for WWAN operation," *Asia Pacific Microwave Conference*, pp. 1987-1989, 2009.
- [8] A. Foudazi, H. R. Hassani, and S. M. A. Nezhad, "Small UWB planar monopole antenna with added GPS/GSM/WLAN bands," *IEEE Transactions on Antennas and Propagation*, vol. 60, no. 6, pp. 2987-2992, June 2012.
- [9] Ansoft High Frequency Structure Simulation (HFSS), ver. 11, Ansoft Corporation, Pittsburgh, PA, USA, 2010.
- [10] CST Microwave Studio, 3D EM Simulation of High Frequency Components, Darmstadt, Germany, 2011.



**Bahadır S. Yıldırım** received his M.Sc. and Ph.D. degrees from the University of Colorado at Boulder, USA, and Arizona State University, Tempe, USA, in 1994 and 1998, respectively. He is currently an Associate Professor in the Dept. of Electrical and Electronics

Engineering at Muğla Sıtkı Koçman University, Muğla, Turkey. His current research interests include antenna design for mobile equipment, computational electromagnetics, RF/microwave amplifiers, wireless power transmission, and pulsed power electronics.



**Erkul Basaran** received the B.S. degree in Electrical and Electronics Engineering from the Selcuk University, Turkey, in 2000, the M.S. and the Ph.D. degree in Electronics Engineering from the Gebze Technical University, Turkey, in 2002 and 2008, respectively.

Until 2015, he was with the Scientific and Technical

Research Council of Turkey (TUBITAK) as a Senior and a Chief Researcher. He is currently an Assistant Professor in the Department of Electrical and Electronics Engineering at Piri Reis University, Turkey. He is interested in computational electromagnetics and acoustics, radar cross section prediction and measurement, microwave component and antenna design.



**Bahattin Türetken** has received M.Sc. and Ph.D. degrees from Istanbul Technical University, Istanbul, Turkey in 1998 and 2002, respectively. He has been working as Chief Researcher at TUBITAK-UEKAE (National Research Institute of Electronics and Cryptology) EMC & TEMPEST Test Center in 1998-2009. He

managed Electromagnetic and Research Group (EMARG) and the project of Antenna Test and Research Center between 2009 and 2012. He has been the Director of “Millimeter and Terahertz Technologies Research Laboratories (MILTAL)” between 2012-2015. His research topics are radar, antenna design and testing, computational electromagnetic, diffraction & scattering EM Problems, civilian and military EMC/EMI problems, terahertz applications, radiometry, biomedical imaging, implant devices. He is the author and co-author of 1 book chapter and over 100 published papers and proceedings in national and international journals and conferences.